

This article was downloaded by: [Renmin University of China]

On: 13 October 2013, At: 10:27

Publisher: Taylor & Francis

Informa Ltd Registered in England and Wales Registered Number: 1072954 Registered office: Mortimer House, 37-41 Mortimer Street, London W1T 3JH, UK



## Journal of Coordination Chemistry

Publication details, including instructions for authors and subscription information:

<http://www.tandfonline.com/loi/gcoo20>

### Effect of the guest solvent molecules on preparation of different morphologies of ZnO nanomaterials from the $[\text{Zn}_2(1,4\text{-bdc})_2(\text{dabco})]$ metal-organic framework

Kamran Akhbari<sup>a</sup> & Ali Morsali<sup>a</sup>

<sup>a</sup> Department of Chemistry, Faculty of Sciences, Tarbiat Modares University, P.O. Box 14155-4838, Tehran, Islamic Republic of Iran

Published online: 06 Oct 2011.

To cite this article: Kamran Akhbari & Ali Morsali (2011) Effect of the guest solvent molecules on preparation of different morphologies of ZnO nanomaterials from the  $[\text{Zn}_2(1,4\text{-bdc})_2(\text{dabco})]$  metal-organic framework, Journal of Coordination Chemistry, 64:20, 3521-3530, DOI:

[10.1080/00958972.2011.623778](https://doi.org/10.1080/00958972.2011.623778)

To link to this article: <http://dx.doi.org/10.1080/00958972.2011.623778>

PLEASE SCROLL DOWN FOR ARTICLE

Taylor & Francis makes every effort to ensure the accuracy of all the information (the "Content") contained in the publications on our platform. However, Taylor & Francis, our agents, and our licensors make no representations or warranties whatsoever as to the accuracy, completeness, or suitability for any purpose of the Content. Any opinions and views expressed in this publication are the opinions and views of the authors, and are not the views of or endorsed by Taylor & Francis. The accuracy of the Content should not be relied upon and should be independently verified with primary sources of information. Taylor and Francis shall not be liable for any losses, actions, claims, proceedings, demands, costs, expenses, damages, and other liabilities whatsoever or howsoever caused arising directly or indirectly in connection with, in relation to or arising out of the use of the Content.

This article may be used for research, teaching, and private study purposes. Any substantial or systematic reproduction, redistribution, reselling, loan, sub-licensing, systematic supply, or distribution in any form to anyone is expressly forbidden. Terms &

Conditions of access and use can be found at <http://www.tandfonline.com/page/terms-and-conditions>

## Effect of the guest solvent molecules on preparation of different morphologies of ZnO nanomaterials from the $[\text{Zn}_2(1,4\text{-bdc})_2(\text{dabco})]$ metal-organic framework

KAMRAN AKHBARI and ALI MORSALI\*

Department of Chemistry, Faculty of Sciences, Tarbiat Modares University, P.O. Box 14155-4838, Tehran, Islamic Republic of Iran

(Received 27 May 2011; in final form 30 August 2011)

The host and the apohost framework of  $[\text{Zn}_2(1,4\text{-bdc})_2(\text{dabco})] \cdot 4\text{DMF} \cdot \frac{1}{2}\text{H}_2\text{O}$  ( $\mathbf{1} \cdot 4\text{DMF} \cdot \frac{1}{2}\text{H}_2\text{O}$ ) (1,4-bdc = 1,4-benzenedicarboxylate and dabco = 1,4-diazabicyclo[2.2.2]octane) were used for the preparation of ZnO nanomaterials. With calcination of the host framework of  $\mathbf{1} \cdot 4\text{DMF} \cdot \frac{1}{2}\text{H}_2\text{O}$ , ZnO nanoparticles could be fabricated. By the same process on fully desolvated framework of  $\mathbf{1}$ , ZnO microrods composed of ZnO nanoparticles were formed. These results indicate with removal of the guest solvent from the pores of this metal-organic framework (MOF), nanoparticle agglomeration increases and the role of this MOF in preparation of ZnO nanoparticles was reduced.

*Keywords:* Metal-organic framework; Nanomaterials; Zinc(II) oxide

### 1. Introduction

Metal-organic frameworks (MOFs) represent highly porous materials [1, 2]. Crystal engineering based on MOFs has attracted considerable interest [3]. These porous compounds have potential applications in gas storage and capture, gas or liquid purification, catalysis, sensor devices, or controlled drug release [4, 5]. Numerous reports of zinc coordination polymers with benzenedicarboxylate exist [6–8] but  $[\text{Zn}_2(1,4\text{-bdc})_2(\text{dabco})] \cdot 4\text{DMF} \cdot \frac{1}{2}\text{H}_2\text{O}$  ( $\mathbf{1} \cdot 4\text{DMF} \cdot \frac{1}{2}\text{H}_2\text{O}$ ) (1,4-bdc = 1,4-benzenedicarboxylate, dabco = 1,4-diazabicyclo[2.2.2]octane and DMF = N,N-dimethylformamide) is one of the most recognized MOFs, first reported by Dybtsev *et al.* in 2004 [9]. This MOF has a jungle-gym-type structure in which a 2-D square grid composed of dinuclear  $\text{Zn}_2$  units is bridged by dabco to extend the 2-D layers into a 3-D structure, affording open channels (with an area of  $7.5 \times 7.5 \text{ \AA}^2$ ), large enough to allow passage of small gas molecules. In spite of its fully connected 3-D structure,  $\mathbf{1}$  has enough flexibility to produce three different crystalline forms [10]. Not only gas molecules but also organic vapors such as methanol (MeOH) [11], ethanol (EtOH) [11], iso-propanol (i-PrOH) [10, 11], and acetone ( $\text{Me}_2\text{CO}$ ) [11] can be adsorbed on  $\mathbf{1}$ . The host framework

\*Corresponding author. Email: morsali\_a@modares.ac.ir

shrinks upon inclusion of organic guest molecules and expands upon guest removal [12]; it has an exceptionally high surface area ( $1450 \text{ m}^2 \cdot \text{g}^{-1}$ ) and  $\text{H}_2$  sorption capacity (2.0 wt% at 1 bar) [12]. Sol-gel [13, 14], hydrothermal [13, 14], pyrolysis of appropriate precursor [15], usage of copolymer agents [16], methods etc. were applied in the preparation of ZnO nanomaterials. Zn(II) coordination polymers were used as new precursors for the preparation of ZnO nanomaterials [17–19]. Our search in fabricating nanomaterials from MOFs indicates that other nanomaterials such as Cu nanoparticles from  $[\text{Cu}_3(\text{btc})_2]$  (btc = benzene-1,3,5-tricarboxylate) [12], ZnO nanoparticles from  $\text{Zn}_4\text{O}(1,4\text{-bdc})_3$  [20], 1-D nano ZnO materials from  $[\text{ZnF}(\text{AmTAZ})]$  solvents (AmTAZ = 3-amino-1,2,4-triazole) [21], and PdO nanoparticles from a  $\text{Pd}^{\text{II}}$  MOF, based on tetra-pyridyl porphyrin [22], were prepared; none of these works consider the role of guest solvent molecules in forming nanomaterials from MOFs. Here we report another application of  $1 \cdot 4\text{DMF} \cdot \frac{1}{2}\text{H}_2\text{O}$  in preparation of nano ZnO and consider the guest influence on forming different morphologies of nano ZnO from the host and the apohost frameworks.

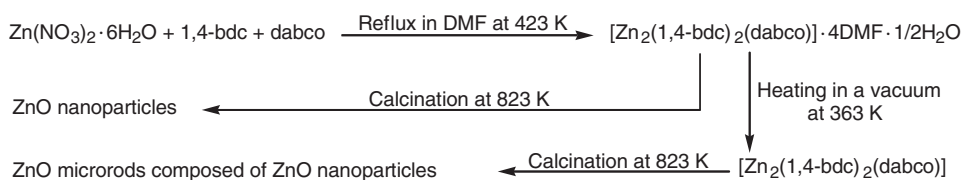
## 2. Experimental

### 2.1. Materials and physical techniques

All reagents and solvents for synthesis and analysis were commercially available from Merck and used as received. Microanalyses were carried out using a Heraeus CHN-O-Rapid analyzer. The thermal behavior was measured with a PL-STA 1500 apparatus between  $40^\circ\text{C}$  and  $610^\circ\text{C}$  in static nitrogen. X-ray powder diffraction (XRD) measurements were performed using an X'pert diffractometer of Philips with monochromated Co-K $\alpha$  radiation ( $\lambda = 1.78897 \text{ \AA}$ ). The samples were characterized with a scanning electron microscope (SEM) (Philips XL 30) with gold coating.

### 2.2. Synthesis of $[\text{Zn}_2(1,4\text{-bdc})_2(\text{dabco})] \cdot 4\text{DMF} \cdot \frac{1}{2}\text{H}_2\text{O}$ , preparation of $[\text{Zn}_2(1,4\text{-bdc})_2(\text{dabco})]$ and ZnO nanostructures from these precursors

White powder of  $[\text{Zn}_2(1,4\text{-bdc})_2(\text{dabco})] \cdot 4\text{DMF} \cdot \frac{1}{2}\text{H}_2\text{O}$  was synthesized according to previous procedures [9, 23] by dissolving 10 g of  $\text{Zn}(\text{NO}_3)_2 \cdot 6\text{H}_2\text{O}$  (33.6 mmol), 5.60 g of 1,4-bdc (33.7 mmol) and 1.87 g of dabco (16.7 mmol) in 100 mL DMF and refluxing the resulting solution at  $150^\circ\text{C}$  for 8 h; 5 h after beginning of the reflux white precipitate formed. After filtering, the white precipitate was washed with DMF and dried at room temperature for 2 days (11.371 g, 78%). Anal. Calcd for  $(1 \cdot 4\text{DMF} \cdot \frac{1}{2}\text{H}_2\text{O})$ : C, 46.80; H, 5.66; N, 9.63. Found (%): C, 47.10; H, 5.52; N, 9.68. White powder of  $[\text{Zn}_2(1,4\text{-bdc})_2(\text{dabco})]$  (**1**) was prepared by heating half of the  $1 \cdot 4\text{DMF} \cdot \frac{1}{2}\text{H}_2\text{O}$  powder in a vacuum at  $90^\circ\text{C}$  for 8 h. To prepare zinc oxide nanostructures, calcination of well scattered powder of  $1 \cdot 4\text{DMF} \cdot \frac{1}{2}\text{H}_2\text{O}$  and **1** microrods as a very thin film were done at  $550^\circ\text{C}$  in a furnace with static atmosphere of air for 5 h. Yields for ZnO nanoparticles prepared from host and apohost frameworks are 89% (1.45 g) and 90% (0.73 g), respectively.



Scheme 1. Two different morphologies of nano ZnO prepared from calcination of the host and apohost frameworks of **1**.

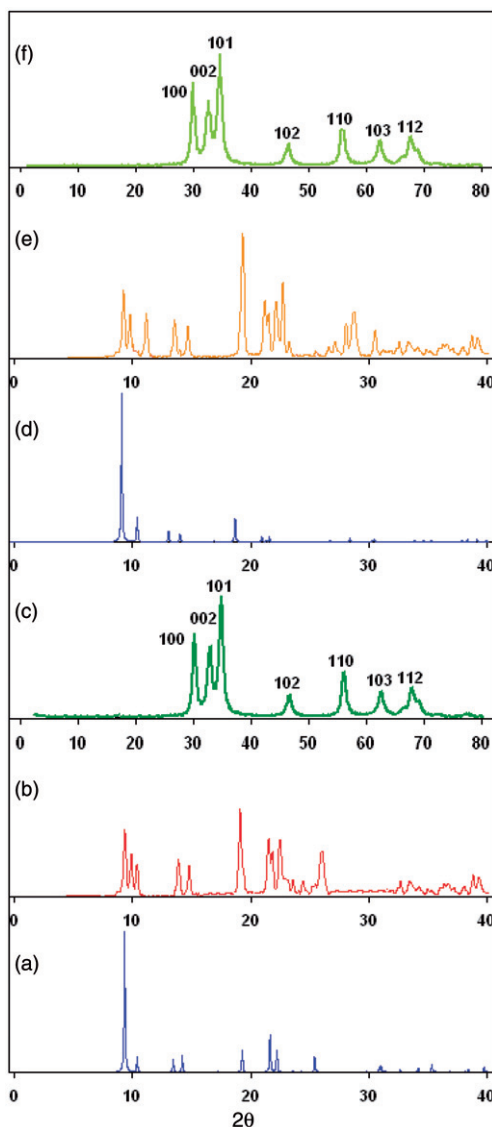


Figure 1. XRD patterns: (a) simulated pattern based on single-crystal data of  $1 \cdot 4\text{DMF} \cdot \frac{1}{2}\text{H}_2\text{O}$ , (b) microrods of  $1 \cdot 4\text{DMF} \cdot \frac{1}{2}\text{H}_2\text{O}$ , (c) ZnO nanoparticles fabricated from calcination of  $1 \cdot 4\text{DMF} \cdot \frac{1}{2}\text{H}_2\text{O}$  microrods, (d) simulated pattern based on single-crystal data of  $[\text{Zn}_2(1,4\text{-bdc})_2(\text{dabco})]$  (**1**), (e) microrods of **1**, and (f) ZnO nanoparticles fabricated from calcination of **1** microrods.

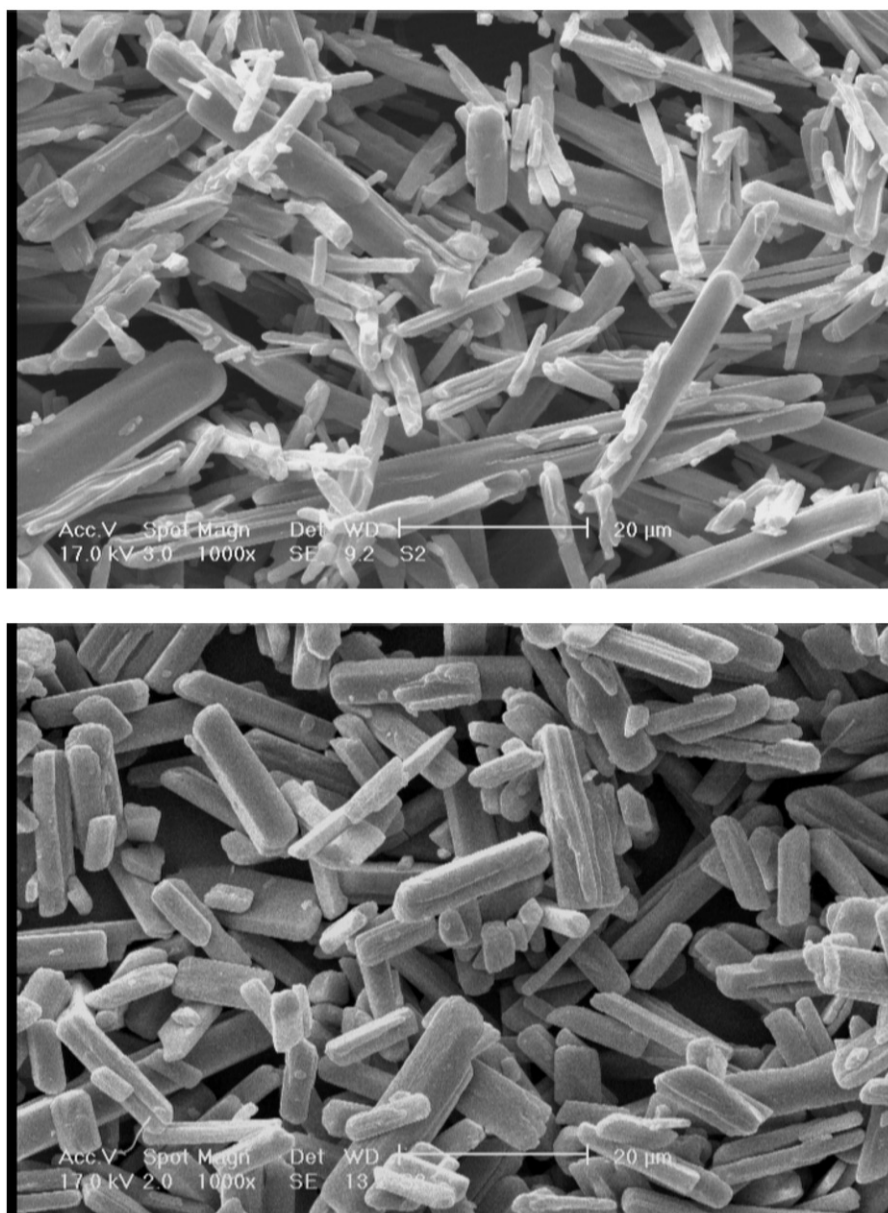


Figure 2. SEM images of  $1 \cdot 4\text{DMF} \cdot \frac{1}{2}\text{H}_2\text{O}$  microrods (top) and **1** microrods after desolvation in a vacuum at  $90^\circ\text{C}$  (bottom).

### 3. Results and discussion

Scheme 1 shows the schematic representation of nano ZnO formation from the host and apohost framework of **1**.

Reaction between 1,4-bdc, dabco, and  $\text{Zn}(\text{NO}_3)_2 \cdot 6\text{H}_2\text{O}$  in DMF under reflux results in the formation of white powder which was dried at room temperature.

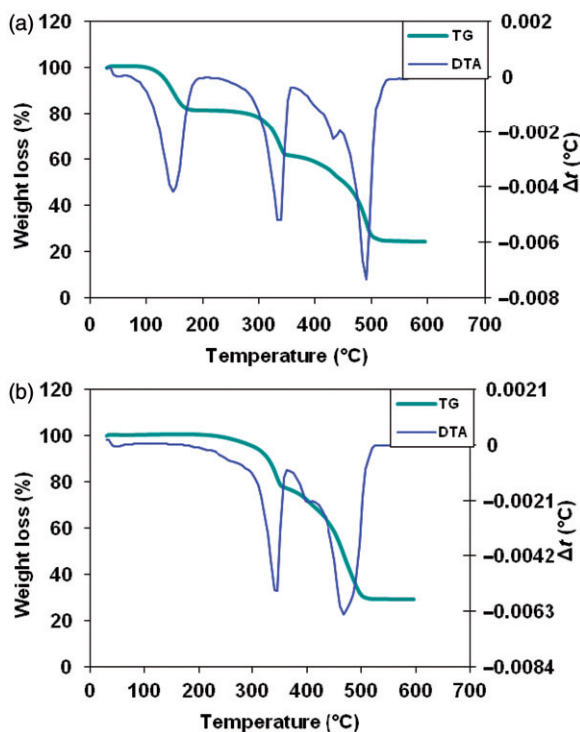


Figure 3. Thermal behavior of  $[\text{Zn}_2(1,4\text{-bdc})_2(\text{dabco})] \cdot 4\text{DMF} \cdot \frac{1}{2}\text{H}_2\text{O}$  ( $1 \cdot 4\text{DMF} \cdot \frac{1}{2}\text{H}_2\text{O}$ , (a)) and  $[\text{Zn}_2(1,4\text{-bdc})_2(\text{dabco})]$  (**1**, (b)).

Comparison between the XRD patterns simulated from single-crystal X-ray data (figure 1a) and that of the powder (figure 1b) proved formation of  $1 \cdot 4\text{DMF} \cdot \frac{1}{2}\text{H}_2\text{O}$ . Figure 2 (top) shows the SEM image of  $1 \cdot 4\text{DMF} \cdot \frac{1}{2}\text{H}_2\text{O}$  microrods. In order to prepare **1** microrods (figure 2 bottom), half of the  $1 \cdot 4\text{DMF} \cdot \frac{1}{2}\text{H}_2\text{O}$  powder was heated in a vacuum at  $90^\circ\text{C}$  for 8 h. The XRD pattern of the resulting powder (figure 1e) matches with the simulated XRD pattern from single-crystal X-ray data (figure 1d).

Figure 3(a) and (b) show the thermogravimetric analysis (TGA) and differential thermal analysis (DTA) of  $1 \cdot 4\text{DMF} \cdot \frac{1}{2}\text{H}_2\text{O}$  and **1**, respectively. The TGA data (figure 3a) indicate that  $1 \cdot 4\text{DMF} \cdot \frac{1}{2}\text{H}_2\text{O}$  loses its guest molecules at  $100\text{--}175^\circ\text{C}$ , and the resulting apohost framework starts to decompose after  $250^\circ\text{C}$ . Besides the XRD pattern of **1** apohost framework (figure 1e), the TGA data of this powder (figure 3b), identical to that of  $1 \cdot 4\text{DMF} \cdot \frac{1}{2}\text{H}_2\text{O}$  after  $250^\circ\text{C}$ , confirm the formation of apohost framework. Thus no guest molecules were left in the porous framework. These TGA data indicate that decomposition of both host and apohost frameworks are complete at  $550^\circ\text{C}$ .

Figure 4 (top) shows the schematic structure of  $1 \cdot 4\text{DMF} \cdot \frac{1}{2}\text{H}_2\text{O}$  framework. A fragment of  $1 \cdot 4\text{DMF} \cdot \frac{1}{2}\text{H}_2\text{O}$  host framework along the crystallographic  $c$ -axis could be observed in figure 4 (middle), which shows that four DMF's are in an imaginary circle of MOF pores. To prepare zinc oxide nanostructures and to consider the role of guest molecules on the formation of different morphologies of zinc oxide



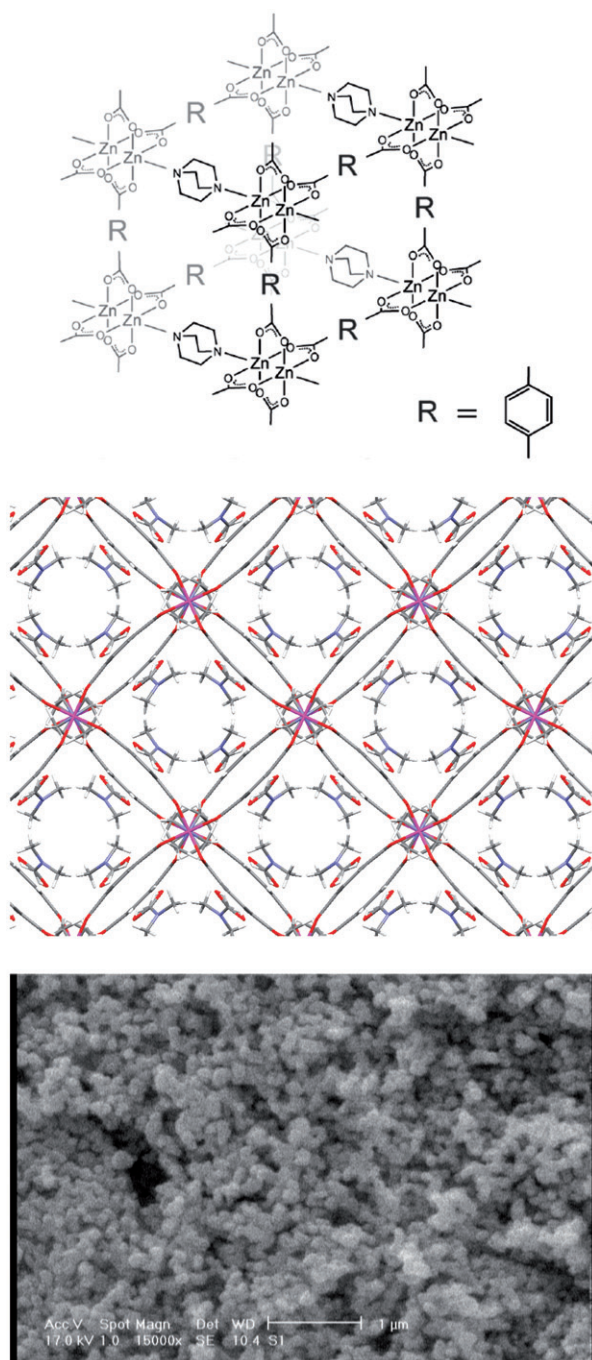


Figure 4. Schematic structure of  $[Zn_2(1,4-bdc)_2(dabco)]$  framework (top), a fragment of the host framework of  $1 \cdot 4DMF \cdot \frac{1}{2}H_2O$  along the crystallographic *c*-axis (middle) and the SEM image of ZnO nanoparticles, fabricated from calcination of  $1 \cdot 4DMF \cdot \frac{1}{2}H_2O$  at  $550^\circ C$  (bottom), (Zn = violet, O = red, C = gray, N = blue and H = white).



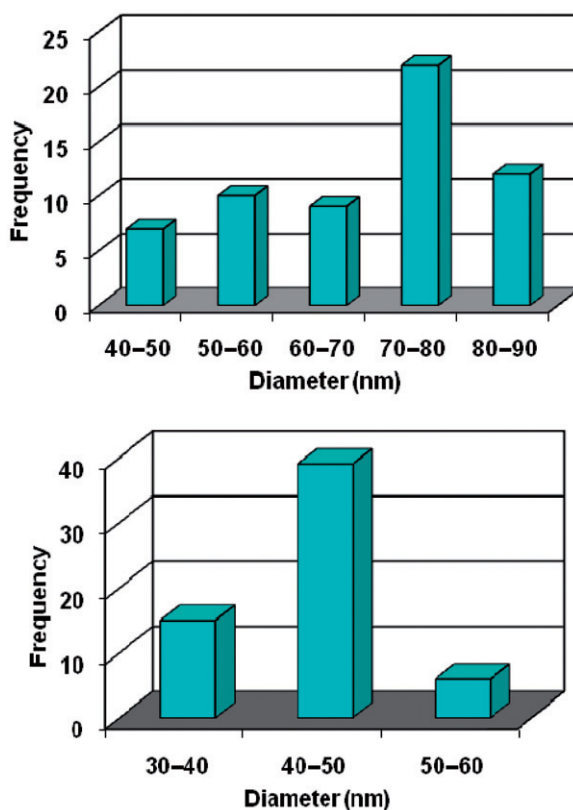


Figure 5. Particle size distribution histograms of ZnO nanoparticles prepared from  $1 \cdot 4\text{DMF} \cdot \frac{1}{2}\text{H}_2\text{O}$  (top) and from the apohost framework of **1** (bottom).

nanostructures, calcination of  $1 \cdot 4\text{DMF} \cdot \frac{1}{2}\text{H}_2\text{O}$  and **1** powders were done at  $550^\circ\text{C}$  in static air.

Figure 1(c) and (f) show the XRD patterns of zinc(II) oxide nanostructures prepared by this process. The XRD pattern is in agreement with the typical wurtzite structure of ZnO (hexagonal phase, space group  $P6_3mc$ , with lattice constants  $a = 3.24982(9) \text{ \AA}$ ,  $c = 1.6021 \text{ \AA}$ ,  $Z = 2$ , JCPDS No. 36-1451). Figure 4 (bottom) and figure S1 show the SEM images of ZnO nanoparticles obtained from the calcination of the  $1 \cdot 4\text{DMF} \cdot \frac{1}{2}\text{H}_2\text{O}$  framework. The corresponding particle size distribution histogram of these nanoparticles is shown in figure 5 (top). These nanoparticles have diameters between 40 and 90 nm, but the frequency (number of nanoparticles in each size distribution) of nanoparticles with 70–80 nm diameter are highest. If we consider the SEM images of ZnO nanostructures, obtained from calcination of **1** (figure 6 (middle, bottom) and figure S2), it is obvious that very different morphologies are obtained (figure 4 bottom). These ZnO nanostructures maintain the original morphology of apohost framework (figure 2 bottom), maintaining microrod structures, but the microrods are fabricated from ZnO nanoparticles (figure 6 bottom).

Calcination of **1** with no solvent in the MOF pores (figure 6 top) results in the removal of the organic parts of the MOF and formation of ZnO microrods of ZnO

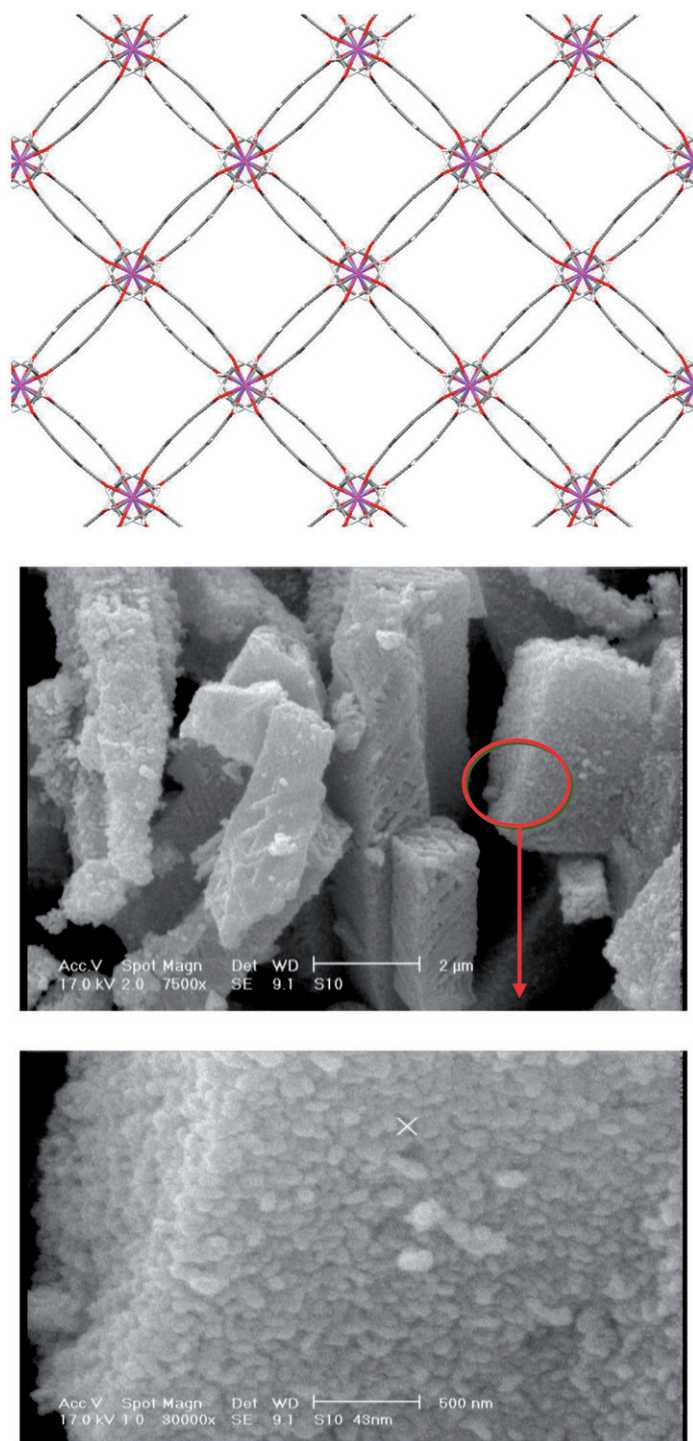


Figure 6. A fragment of the apohost framework of **1** along the crystallographic *c*-axis (top) and the SEM image of ZnO nanoparticles, fabricated from calcination of the apohost framework of **1** at 550°C (middle and bottom), (Zn = violet, O = red, C = gray, N = blue and H = white).

nanoparticles with particle size distribution of 30–60 nm (figure 5 bottom), lower than that observed from the host framework (figure 5 top). The tendency of the ZnO nanoparticles to aggregate is increased. Figure 5 (bottom) also shows that the frequencies of nanoparticles with size distribution of 40–50 nm are higher than others.

Our work indicates that fully solvated MOFs such as  $\mathbf{1} \cdot 4\text{DMF} \cdot \frac{1}{2}\text{H}_2\text{O}$  could be used for the preparation ZnO nanoparticles. The role of organic ligands and solvent in  $\mathbf{1} \cdot 4\text{DMF} \cdot \frac{1}{2}\text{H}_2\text{O}$  MOF is similar to the role of polymer stabilizers in formation of nanoparticles. With the removal of the solvent from the pores of the host framework, the tendency of nanoparticles to agglomerate, due to large specific surface area as well as high surface energy, was increased. Agglomerated microrods of ZnO, composed of ZnO nanoparticles with the same morphology of the apohost material, were formed. Thus loss of DMF and  $\text{H}_2\text{O}$  from the pores of the framework reduces the role of  $\mathbf{1} \cdot 4\text{DMF} \cdot \frac{1}{2}\text{H}_2\text{O}$  MOF in the preparation of nano ZnO. For applications of ZnO nanomaterials such as light-emitting diodes [24], photodetectors [25], photodiodes [26], gas sensors [27], and dye-sensitized solar cells (DSSCs) [28], preparation of ZnO nanomaterials from their MOFs is a simple and effective method.

#### 4. Conclusions

Host and apohost frameworks of  $[\text{Zn}_2(1,4\text{-bdc})_2(\text{dabco})] \cdot 4\text{DMF} \cdot \frac{1}{2}\text{H}_2\text{O}$  were used for the preparation of ZnO nanomaterials. With calcination of the host framework, ZnO nanoparticles could be fabricated. By the same process on the fully desolvated framework of  $\mathbf{1}$ , ZnO microrods composed of ZnO nanoparticles were formed. Due to loss of DMF and  $\text{H}_2\text{O}$  from the pores of the framework in  $\mathbf{1}$  and the tendency of nanoparticles to agglomerate, the role of the MOF in the preparation of nano ZnO was reduced. Thus agglomerated microrods of ZnO, composed of ZnO nanoparticles, with the same morphology of the apohost material, were formed. We conclude that the role of guest DMF in the preparation of ZnO nanoparticles from  $\mathbf{1} \cdot 4\text{DMF} \cdot \frac{1}{2}\text{H}_2\text{O}$  is similar to the role of polymer stabilizers in the formation of nanoparticles.

#### Supplementary material

Electronic supplementary information includes other SEM images of ZnO nanostructures.

#### Acknowledgments

Support of this investigation by Tarbiat Modares University and National Iranian Gas Company is gratefully acknowledged.

## References

- [1] O.M. Yaghi, M. O'Keeffe, N.W. Ockwig, H.K. Chae, M. Eddaoudi, J. Kim. *Nature*, **423**, 705 (2003).
- [2] S. Kitagawa, R. Kitaura, S.-I. Noro. *Angew. Chem. Int. Ed.*, **43**, 2334 (2004).
- [3] B. Chen, S. Xiang, G. Qian. *Acc. Chem. Res.*, **43**, 1115 (2010).
- [4] G. Férey. *Chem. Soc. Rev.*, **37**, 191 (2008).
- [5] R.J. Kuppler, D.J. Timmons, Q.-R. Fang, J.-R. Li, T.A. Makal, M.D. Young, D. Yuan, D. Zhao, W. Zhuang, H.-C. Zhou. *Coord. Chem. Rev.*, **253**, 3042 (2009).
- [6] H. Chang, M. Fu, X.-J. Zhao, E.-C. Yang. *J. Coord. Chem.*, **63**, 3551 (2010).
- [7] D. Feng, S.-X. Liu, P. Sun, F.-J. Ma, W. Zhang. *J. Coord. Chem.*, **63**, 1737 (2010).
- [8] X. Lu, Y.-Y. Chen, P.-Z. Li, Y.-G. Bi, C. Yu, X.-D. Shi, Z.-X. Chi. *J. Coord. Chem.*, **63**, 3923 (2010).
- [9] D.N. Dybtsev, H. Chun, K. Kim. *Angew. Chem. Int. Ed.*, **43**, 5033 (2004).
- [10] K. Uemura, Y. Yamasaki, Y. Komagawa, K. Tanaka, H. Kita. *Angew. Chem. Int. Ed.*, **46**, 6662 (2007).
- [11] K. Uemura, Y. Komagawa, Y. Yamasaki, H. Kita. *Desalination*, **234**, 1 (2008).
- [12] L. Chen, Y. Shen, J. Bai, C. Wang. *J. Solid State Chem.*, **182**, 2298 (2009).
- [13] M. Xingfa, L. Aiyun, X. Huizhong, L. Guang, H. Meng, W. Gang. *Curr. Nanosci.*, **4**, 157 (2008).
- [14] K.S. Kim, H. Jeong, M.S. Jeong, G.Y. Jung. *Adv. Funct. Mater.*, **20**, 3055 (2010).
- [15] F. Xu, M. Dai, Y. Lu, L. Sun. *J. Phys. Chem. C*, **114**, 2776 (2010).
- [16] C. Ge, Z. Bai, M. Hu, D. Zeng, S. Cai, C. Xie. *Mater. Lett.*, **62**, 2307 (2008).
- [17] B. Luo, W.L. Gladfelter. *J. Coord. Chem.*, **64**, 82 (2011).
- [18] Z. Rashidi Ranjbar, A. Morsali. *Ultrason. Sonochem.*, **18**, 644 (2011).
- [19] M. Khanpour, A. Morsali, P. Retailleau. *Polyhedron*, **29**, 1520 (2010).
- [20] L. Zhang, Y.H. Hu. *J. Phys. Chem. C*, **114**, 2566 (2010).
- [21] C.-Y. Su, A.M. Goforth, M.D. Smith, P.J. Pellechia, H.-C. Loye. *J. Am. Chem. Soc.*, **126**, 3576 (2004).
- [22] V. Bagchi, D. Bandyopadhyay. *J. Organomet. Chem.*, **694**, 1259 (2009).
- [23] K. Uemura, Y. Komagawa, Y. Yamasaki, H. Kita. *Desalination*, **234**, 1 (2008).
- [24] N. Saito, H. Haneda, T. Sekiguchi, N. Ohashi, I. Sakaguchi, K. Koumoto. *Adv. Mater.*, **14**, 418 (2002).
- [25] S. Liang, H. Sheng, Y. Liu, Z. Hio, Y. Lu, H. Shen. *J. Cryst. Growth*, **225**, 110 (2001).
- [26] J.Y. Lee, Y.S. Choi, J.H. Kim, M.O. Park, S. Im. *Thin Solid Films*, **403**, 553 (2002).
- [27] N. Golego, S.A. Studenikin, M. Cocivera. *J. Electrochem. Soc.*, **147**, 1592 (2000).
- [28] C. Bauer, G. Boschloo, E. Mukhtar, A. Hagfeldt. *J. Phys. Chem. B*, **105**, 5585 (2001).